iScience

CellPress
OPEN ACCESS

Article

# Neuropeptide F inhibits dopamine neuron interference of long-term memory consolidation in *Drosophila*

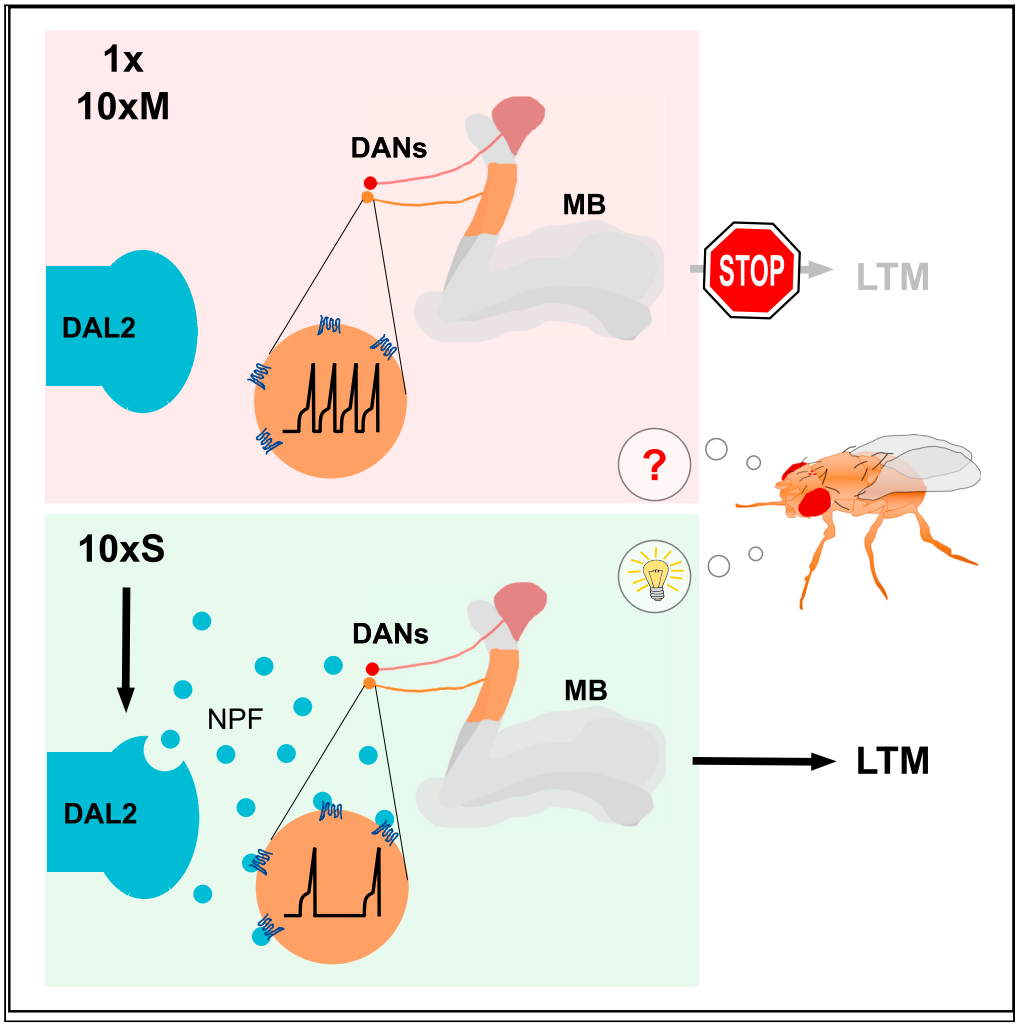


Kuan-Lin Feng, Ju-Yun Weng, Chun-Chao Chen, ..., Tim Tully, Cheng-Chang Lien, Ann-Shyn Chiang

cclien@ym.edu.tw (C.-C.L.)
aschiang@life.nthu.edu.tw (A.-S.C.)

## Highlights

Specific dopaminergic neurons interfere with long-term memory (LTM) consolidation

NPF signaling to these dopaminergic neurons is required for LTM formation

Training-induced NPF from a pair of neurons suppresses dopaminergic neurons

NPF signaling acts as a disinhibitory gate for LTM consolidation

Feng et al., iScience *24*, 103506
December 17, 2021 
https://doi.org/10.1016/j.isci.2021.103506

iScience

CellPress
OPEN ACCESS

Article

# Neuropeptide F inhibits dopamine neuron interference of long-term memory consolidation in *Drosophila*

Kuan-Lin Feng,[1,12] Ju-Yun Weng,[2,12] Chun-Chao Chen,[2] Mohammed Bin Abubaker,[2] Hsuan-Wen Lin,[2] Ching-Che Charng,[3] Chung-Chuan Lo,[2,3] J. Steven de Belle,[2,4,5,6] Tim Tully,[1,2] Cheng-Chang Lien,[7,*] and Ann-Shyn Chiang[1,2,3,8,9,10,11,13,*]

## SUMMARY

**Long-term memory (LTM) formation requires consolidation processes to overcome interfering signals that erode memory formation. Olfactory memory in *Drosophila* involves convergent projection neuron (PN; odor) and dopaminergic neuron (DAN; reinforcement) input to the mushroom body (MB). How post-training DAN activity in the posterior lateral protocerebrum (PPL1) continues to regulate memory consolidation remains unknown. Here we address this question using targeted transgenes in behavior and electrophysiology experiments to show that (1) persistent post-training activity of PPL1-α2α′2 and PPL1-α3 DANs interferes with aversive LTM formation; (2) neuropeptide F (NPF) signaling blocks this interference in PPL1-α2α′2 and PPL1-α3 DANs after spaced training to enable LTM formation; and (3) training-induced NPF release and neurotransmission from two upstream dorsal-anterior-lateral (DAL2) neurons are required to form LTM. Thus, NPF signals from DAL2 neurons to specific PPL1 DANs disinhibit the memory circuit, ensuring that periodic events are remembered as consolidated LTM.**

## INTRODUCTION

Memory is an adaptive property of the nervous system that confers an ability to predict environmental features of varying consequence and periodicity (Nairne et al., 2007). Salient, regular, and thus meaningful memories may be consolidated into persistent forms, whereas others are forgotten (McGaugh, 1966). Long-term memory (LTM) consolidation requires enduring biological processes at molecular, cellular, and circuitry levels of organization to form "traces" in memory-encoding neurons (Tonegawa et al., 2018). A balance between the stabilization and erosion of these traces is reflected as different phases of retained memory (Davis and Zhong, 2017). Identified dopaminergic neurons (DAN) in the *Drosophila* brain that signal reinforcement during aversive olfactory learning (Aso et al., 2012; Qin et al., 2012; Aso and Rubin, 2016) may also interfere with the formation of short- and intermediate-term memories (STM and ITM, respectively) if these neurons remain persistently active (Berry et al., 2012). This forms our hypothesis that DAN-mediated interference is a key factor regulating or "gating" memory traces into either transient or stabilized forms, ultimately influencing LTM consolidation.

In *Drosophila*, consolidated LTM can be formed by Pavlovian conditioning, whereby presentations of an odor (conditioned stimulus, CS) paired with a punishment or reward (unconditioned stimuli, US) can trigger protein synthesis-dependent cellular events in specific brain circuit elements. Aversive LTM typically requires recurrent paired presentations (Tully et al., 1994), whereas appetitive LTM can be formed by a single training cycle (Krashes and Waddell, 2008). Typically, behavioral metrics of consolidation, storage, and retrieval are the conditioned responses persisting for at least 24 h post-training. Sensory and reinforcement signals delivered by projection neurons (PN) and DANs, respectively, are associated by their temporal convergence on mushroom body (MB) intrinsic Kenyon cells (KC) (Aso et al., 2012; Schwaerzel et al., 2003). During learning, DAN output activates postsynaptic Dop1R1 receptors in KCs, leading to depression of signaling at synapses between KCs and mushroom body output neurons (MBONs) (Séjourné et al., 2011, Qin et al., 2012; Hige et al., 2015; Perisse et al., 2016; Handler et al., 2019).

[1]Institute of Biotechnology, National Tsing Hua University, Hsinchu 30013, Taiwan

[2]Brain Research Center, National Tsing Hua University, Hsinchu 30013, Taiwan

[3]Institute of Systems Neuroscience and Department of Life Science, National Tsing Hua University, Hsinchu 30013, Taiwan

[4]Department of Psychological Sciences, University of San Diego, San Diego, CA 92110, USA

[5]School of Life Sciences, University of Nevada, Las Vegas, NV 89154, USA

[6]MnemOdyssey LLC, Escondido, CA 92027, USA

[7]Institute of Neuroscience and Brain Research Center, National Yang Ming Chiao Tung University, Taipei 11221, Taiwan

[8]Kaohsiung Medical University, Kaohsiung 80708, Taiwan

[9]National Health Research Institutes, Zhunan 35053, Taiwan

[10]China Medical University, Taichung 40402, Taiwan

[11]Kavli Institute for Brain and Mind, University of California at San Diego, La Jolla, CA 92093-0526, USA

[12]These authors contributed equally

[13]Lead contact

*Correspondence: cclien@ym.edu.tw (C.-C.L.), aschiang@life.nthu.edu.tw (A.-S.C.)

https://doi.org/10.1016/j.isci.2021.103506

Recent studies reveal that DANs have additional post-training roles in memory formation. Persistent calcium ($Ca^{2+}$) dynamics in two types of DANs in the protocerebral posterior lateral region of the fly brain (PPL1-γ1pedc and PPL1-γ2α′1) appear to positively regulate consolidation of aversive LTM (Plaçais et al., 2012). Alternatively, post-training activity of DANs in the protocerebral anterior medial (PAM) region appear necessary for consolidation of appetitive LTM (Ichinose et al., 2015). Another striking finding is that PPL1-γ1pedc and -γ2α′1 DANs also appear to promote forgetting of transient memory (Berry et al., 2012). Their persistent activity erodes STM and anesthesia-resistant memory (ARM) and favors the consolidation of LTM (Berry et al., 2012, 2015; Plaçais et al., 2012). Comparably lower levels of dopamine released from PPL1 DANs activate another type of postsynaptic KC dopamine receptor, Dop1R2, to potentiate synapses that were previously depressed during learning, leading to a decay of transient memory (Berry et al., 2012; Cervantes-Sandoval et al., 2016, 2020; Handler et al., 2019; Himmelreich et al., 2017). In addition, Dop1R2 receptor activation of Rac1 protein in KCs was previously found to interfere with memory formation by disrupting the cytoskeletal organization induced by learning (Shuai et al., 2010; Cervantes-Sandoval et al., 2016). Overall, DAN involvement in memory formation is multifaceted. Apart from the initial reinforcement signaling during learning that can lead to LTM (Aso et al., 2012; Aso and Rubin, 2016; Qin et al., 2012), persistent DAN activity is implicated in bidirectional regulation of memory formation in *Drosophila* (Berry et al., 2018; Handler et al., 2019). DAN activity may be an integral aspect of systems LTM consolidation, whereby dopamine signaling after initial learning can either promote or interfere with the process.

A candidate modulator of post-training DAN activity is neuropeptide F (NPF), a homologue of mammalian neuropeptide Y (NPY) (Brown et al., 1999). NPF has been shown to regulate processes that influence LTM in *Drosophila*, such as motivation, energy metabolism, circadian timing, and sleep (Krashes et al., 2009; Donlea et al., 2011; Chung et al., 2017; Plaçais et al., 2017; Dag et al., 2019; Chouhan et al., 2021). Of relevance here is the role NPF plays in signaling hunger, motivating food-seeking behavior, and enabling retention of sugar-reward memory in hunger-motivated flies (Krashes et al., 2009; Tsao et al., 2018; Lin et al., 2019). Several studies also link NPF with DAN activity. For example, stimulation of NPF-expressing neurons and blocking memory-inhibiting PPL1-γ1pedc output were shown to promote the retention of reward memory in food-satiated flies (Krashes et al., 2009). In addition, downregulating NPF receptors (NPFRs) in multiple DANs was shown to impair food-seeking behavior (Tsao et al., 2018). Based on these observations that demonstrate the importance of NPF in modulating appetitive behavior, we were interested to know whether NPF may also modulate DAN activity in aversive LTM consolidation.

Among NPF-immunopositive neurons in the brain, we identified one pair of dorsal-anterior-lateral neurons (DAL2) that expresses strong NPF signals and project axons to the dendritic fields of PPL1 DAN neurons. DAL2 neurons are anatomically similar to another pair of DAL neurons that are essential for LTM consolidation, storage, and retrieval in *Drosophila* (Chen et al., 2012; Lin et al., 2021). Our experiments show that the post-training activity of PPL1 DANs results in consolidation failure, whereas spaced training activates NPF signaling from DAL2 neurons to inhibit PPL1 DANs and promote LTM consolidation.

## RESULTS

### Post-training PPL1 DAN activity bidirectionally regulates aversive LTM

Aversive odor learning relies on PPL1-DAN activity, and the decay of subsequent transient STM and ITM phases is promoted by persistent activity of these same neurons and their postsynaptic partners (Berry et al., 2012). Whether post-training PPL1 DAN activity has a role in regulating the consolidation of aversive LTM is unknown. We examined this question by manipulating PPL1 DANs using the neuron-specific split *Gal4* driver *MB504B* (Figure 1A) to ectopically express two temperature-sensitive proteins: dynamin (*shibire$^{ts}$*, *shi$^{ts}$*), which blocks synaptic output (Dubnau et al., 2001), and TrpA1 (*transient receptor potential channel A1*, *TrpA1*), which elevates neuron activity (Viswanath et al., 2003)—in both cases, after a temperature shift to ≥30°C.

First, we showed that *MB504B* expresses Gal4 in four types of DANs: PPL1-γ1pedc, PPL1-γ2α′1, PPL1-α2α′2, and PPL1-α3 DANs (Figure 1A). We then observed enhanced LTM generated with 10 cycles of spaced training (10×S) after blocking the output of these DANs during consolidation in flies expressing *shi$^{ts}$* at a restrictive temperature (32°C) compared with flies carrying either the *Gal4* or *shi$^{ts}$* transgenes alone ($p < 0.05$) (Figure 1B) or in 10×S-trained flies maintained at a permissive temperature (20°C) throughout the experiment (Figure 1C). This effect was specific to LTM since 1-day ARM after 10 cycles of massed training (10×M) was not affected by the same manipulation (Figure 1D).

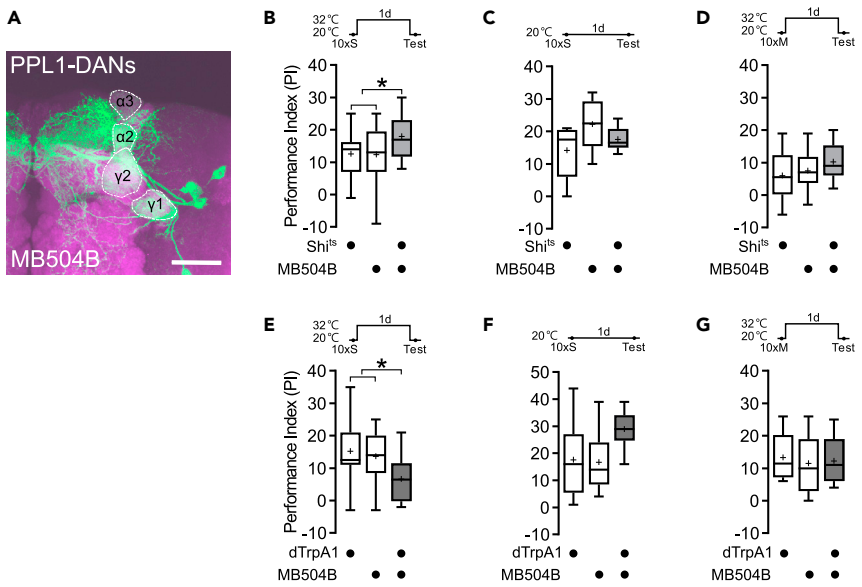


**Figure 1. Post-training PPL1 DAN activity bidirectionally regulates aversive LTM**

(A) *MB504B* > *UAS-mCD8::GFP* labeling of PPL1-γ1pedc, PPL1-γ2α′1, PPL1-α2α′2, and PPL1-α3 DANs (green) counterstained with anti-DLG immunostaining (magenta). Scale bar, 50 μm.

(B) Blocking output from PPL1 DANs in *MB504B* > *UAS-shi$^{ts}$* flies during consolidation elevated 1-day memory after 10×S training ($n$ = 20–22).

(C) Memory was unaffected in these flies after 10×S when neuronal output was not blocked at 20°C ($n$ = 8).

(D) Blocking PPL1 DAN output during consolidation had no effect on 1-day memory after 10×M training ($n$ = 8–14).

(E) Activating PPL1 DANs in *MB504B* > *UAS-dTrpA1* flies during consolidation impaired 1-day memory after 10×S training ($n$ = 12–13).

(F) Memory was unaffected in these flies after 10×S when neuronal output was not activated at 20°C ($n$ = 8–9).

(G) Activating PPL1 DANs during consolidation had no effect on 1-day memory after 10×M training ($n$ = 8–9). Flies were raised at 20°C and shifted to 32°C (restrictive temperature) between training and testing to block dynamin function and synaptic output (B and D) or to elevate TrpA1 channel and neuron activity (E and G) during consolidation. In all figures, temperature control schedules are indicated (top). Box-and-whisker plots show the range of individual data points (whiskers), interquartile spread (box), median (bisecting line), and mean (+). Analysis of variance (ANOVA) was used for all comparisons and Student-Newman-Keuls (SNK) when significant (B and E). *$p < 0.05$.

In contrast, we observed reduced 1-day LTM after elevating DAN activity during consolidation in flies expressing *TrpA1* at 32°C ($p < 0.05$) (Figures 1E and 1F), whereas this manipulation had no effect on ARM (Figure 1G). Together, these results show that aversive memory traces are sensitive to post-training DAN activity during consolidation to LTM.

## Aversive LTM formation requires inhibitory NPF signaling to PPL1 DANs

Because the activity of PPL1 DANs during consolidation negatively correlated with aversive 1-day memory retention (Figure 1), we posited that 10×S training may induce presynaptic release of neurotransmitters or neuromodulators to reduce post-training inhibitory activity of PPL1 DANs, thus enabling the formation of stable LTM. This aligns with a previous finding that NPF inhibition of PPL1-γ1pedc DANs is required during the formation of food-associated olfactory memory when flies are in a hunger state (Krashes et al., 2009).

Before examining aversive memory, we first tested whether NPF can modulate PPL1 DAN membrane potentials using *ex vivo* whole-cell current clamp recording (Figure 2A). PPL1-γ1pedc, -γ2α′1, -α2α′2, and -α3 DANs were labeled by Gal4 encoded by *MB320C*, *MB296B*, *MB058B*, and *MB630B* drivers, respectively. Using bath applications of synthesized NPF we observed hyperpolarization in all four types of PPL1 DANs (Figures 2B–2F), indicating that NPF inhibits these neurons. Although this result may not faithfully reflect the number or density of NPF receptors (NPFR) on the downstream membrane, it is consistent with a previous report of NPFR activation of $K^+$ channels, leading to hyperpolarized membrane potentials (Reale et al., 2004).

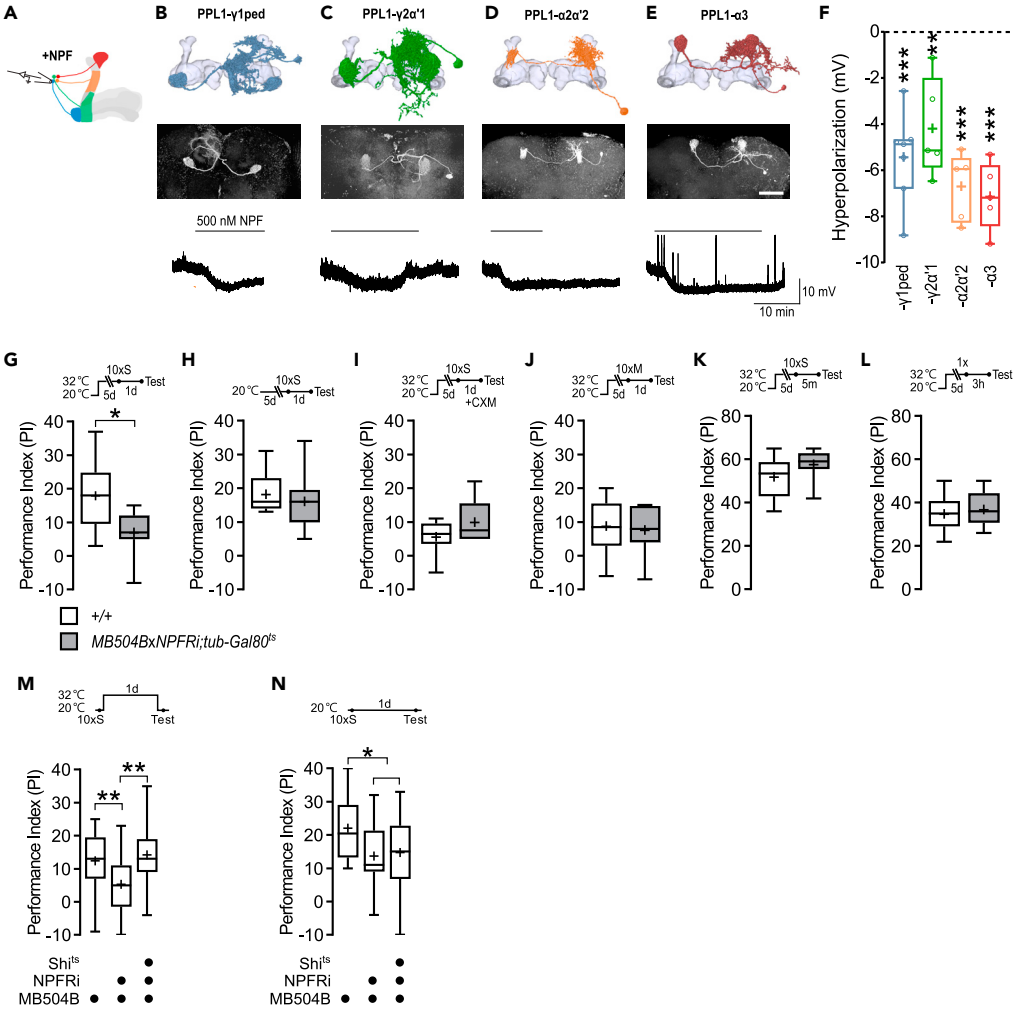


**Figure 2. Aversive LTM formation requires inhibitory NPF signaling to PPL1 DANs**

(A) Schematic of current-clamp recording of four types of PPL1 DANs.

(B–E) Morphologies of PPL1 DANs (FlyCircuit database) (top). *Post-hoc* staining of recorded PPL1 DANs (middle). Scale bar, 50 μm. Representative traces of tested PPL1 DANs upon bath application of 500 nM NPF (bottom). Membrane potential was initially maintained at −60 mV by injecting negative current. The same negative current was applied consistently during the recording.

(F) Quantification of hyperpolarized membrane potentials compared with the baseline before NPF application ($n$ = 5–7).

(G) Adult-stage-specific downregulation of *NPFR* targeted to all PPL1 DANs in *MB504B* > *UAS-NPFRi; tub-Gal80$^{ts}$* flies impaired 1-day memory after 10×S training ($n$ = 10–11). Flies were raised at 20°C and transferred to 32°C to remove Gal4 inhibition by *tub-Gal80$^{ts}$* for 5 days before training.

(H) Memory was unaffected after 10×S when *NPFR RNAi* was not induced in these flies at 20°C ($n$ = 9–11).

(I) LTM reduction after acute *NPFR* downregulation in PPL1-DANs was not further impaired by CXM feeding ($n$ = 8).

(J) Acute *NPFR* downregulation in PPL1 DANs had no effect on 1-day memory after 10×M training ($n$ = 8–12).

(K) The same manipulation did not affect 5-min memory after 10×S training ($n$ = 8).

(L) Similarly, this manipulation did not affect 3-h memory after 1× training ($n$ = 8–10).

(M) Acute dynamin$^{ts}$ (*shi$^{ts}$*) expression in PPL1 DANs blocked signaling from these neurons during consolidation at 32°C, rescuing 1-day memory after 10×S training that was otherwise impaired by *NPFR* downregulation ($n$ = 20–23). Flies were raised at 20°C and transferred to 32°C for temporal control of the *UAS-shi$^{ts}$* transgene.

(N) We observed a 1-day memory deficit after 10×S training in uninduced *MB504B* > *UAS-NPFRi;UAS-shi$^{ts}$* flies maintained at 20°C that was not rescued by *UAS-shi$^{ts}$* transgene expression in PPL1 DANs ($n$ = 20–22). Temperature control schedules are indicated (top). Box-and-whisker plots show the range of individual data points (whiskers), interquartile spread (box), median (bisecting line), and mean (+). t tests were used for all comparisons except (M and N), compared using ANOVA and SNK. *p < 0.05; **p < 0.01; ***p < 0.001. See also Figure S1.

We next tested whether NPF-mediated PPL1 DAN inhibition was necessary for consolidating aversive LTM using *MB504B* to drive RNAi downregulation of NPFRs in these four DANs. The efficacy of *NPFR RNAi* was verified by immunostaining with NPFR antibody (Figure S1). Temporal control of the *UAS-NPFRi* transgene was enabled using a *tub-Gal80$^{ts}$* transgene (conditional expression of Gal80 suppresses Gal4 expression at 20°C but not above 30°C) (McGuire et al., 2003). We found impaired 1-day memory after 10×S training in these flies at 32°C ($p < 0.05$) (Figure 2G) but not at 20°C (Figure 2H). This systemic impairment appeared to be complete, because 1-day memory was not further reduced by feeding flies with the protein synthesis inhibitor cycloheximide (CXM) (Figure 2I). Moreover, NPFR downregulation at 32°C was specific to LTM because we saw no effects on 1-day ARM after 10×M training (Figure 2J), on 5-min STM after 10×S (Figure 2K), or on 3-h ITM after 1× training (Figure 2L). As we are limited by the temporal resolution of RNAi downregulation, the effect of NPFR knockdown persisted through all the memory phases. Our results suggest that memory impairment in flies lacking NPFRs was due to elevated post-training activity of PPL1 DANs.

We reasoned that blocking PPL1 DAN output during consolidation (between training and testing) might rescue the LTM impairment resulting from loss of NPF signaling (Figure 2G). To test the idea, we used *MB504B* to co-express *NPFR RNAi* and *shi$^{ts}$* in PPL1 DANs to block both NPF signaling and neurotransmission during memory consolidation. As expected, blocking DAN output at the restrictive temperature (32°C) overcame the loss of *NPF* signaling and rescued 1-day LTM ($p < 0.05$) (Figure 2M), whereas at the permissive temperature (20°C) 1-day LTM remained impaired ($p < 0.05$) (Figure 2N). These results showed that inhibitory NPF signaling is required to block PPL1 DAN neurotransmission during aversive LTM consolidation.

## NPF-mediated inhibition of two types of PPL1 DANs is required for LTM formation

As different types of PPL1 DANs are known to participate in forming distinct phases of memory (Aso and Rubin, 2016), we suspected that NPF signaling may regulate memory formation by modulating specific PPL1 DANs. We addressed this idea by downregulating NPFRs in each of the four PPL1 DAN types (Figures 3A, 3D, 3G, and 3J) using RNAi- and DAN-specific driver transgenes (see Figure 2). LTM was not affected by inhibiting NPFR expression in PPL1-γ1pedc and -γ2α′1 DANs (Figures 3B and 3E). However, we observed significantly reduced LTM by inhibiting NPFRs in PPL1-α2α′2, and -α3 DANs, at a restrictive temperature (32°C) (Figures 3H and 3K; $p < 0.05$) in comparison with flies maintained at a permissive temperature (20°C) throughout the experiment (Figure 3M). Furthermore, inhibition of NPFRs in PPL1-α3 DANs had no effect on learning after 1× (Figure 3N) or 3-h memory after 1× training (Figure 3O). Although a similar NPFR inhibition in PPL1-α2α′2 DANs also did not affect learning (Figure 3N), these flies showed enhanced 3-h memory after 1× training when NPFRs were inhibited at 32°C ($p < 0.05$) (Figure 3O). However, this enhancement may not have been dependent on NPF signaling because uninduced flies held at 20°C throughout the experiment had similar performance ($p < 0.05$) (Figure 3P).

For comparison and in parallel with these experiments, we recorded spontaneous firing frequencies of each type of PPL1 DAN with and without RNAi downregulation of NPFRs (Figure S2). Effects of 10×S training and NPF signaling in PPL1-γ1pedc, -γ2α′1, and -α3 DANs were not significant (Figures 3C, 3F, and 3L). Spiking was, however, depressed in PPL1-α2α′2 DANs of wild-type flies in comparison with NPFR-inhibited flies after 10×S training ($p < 0.05$) (Figure 3I, left). This difference was not seen among naïve flies (Figure 3I, right), suggesting that NPF signaling was activated by 10×S training, which then inhibited PPL1-α2α′2 DAN output (Figure 3I). Although we observed a similar trend in the depression of wild-type PPL1-α3 DAN spiking in comparison with NPFR-inhibited flies after 10×S training, the differences were not significant (Figure 3L). These results show that 10×S training-induced NPF signaling inhibits post-training activity of two types of DANs (PPL1-α2α′2 and probably -α3) and that this inhibition by NPF is necessary for the formation of aversive LTM.

## Training-induced NPF signaling from DAL2 neurons inhibits PPL1 DANs

To identify the upstream source of spaced training-induced NPF release, we first examined the expression pattern of *NPF* promoter-driven *Gal4* in fly brains using immunostaining for NPF. The *NPF-Gal4* expression pattern revealed several cell bodies in the anterior dorsolateral protocerebrum and the posterior medial protocerebrum. Notably, two pairs of neurons showed strong NPF expression (Figure S3A). One pair, hereafter named dorsal-anterior-lateral-two (DAL2) neurons, are located near another DAL neuron pair that are critical for memory encoding (Chen et al., 2012). DAL2 neurites were found to arborize in the superior

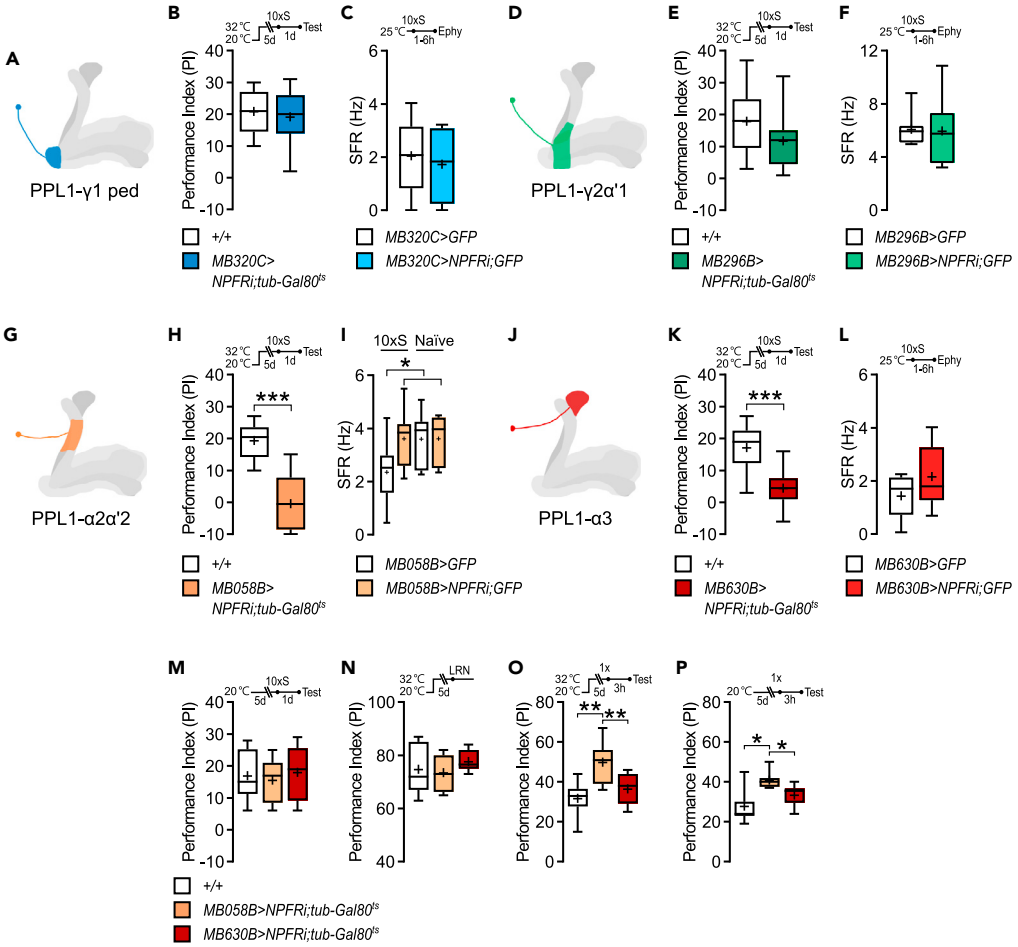


**Figure 3. NPF-mediated inhibition of two types of PPL1 DANs is required for LTM formation**

(A) PPL1-γ1pedc DAN schematic.

(B) Acute *NPFR* downregulation targeted to PPL1-γ1pedc neurons in *MB320C > UAS-NPFRi; tub-Gal80$^{ts}$* flies did not affect 1-day memory when shifted to 32°C after 10×S training ($n$ = 13–15).

(C) Constitutive *NPFR* downregulation targeted to PPL1-γ1pedc neurons in *MB320C > UAS-NPFRi; UAS-GFP* flies did not affect spontaneous firing rate (SFR) after 10×S training ($n$ = 8–9).

(D) PPL1-γ2α′1 DAN schematic.

(E) Acute *NPFR* downregulation in PPL1-γ2α′1 neurons targeted by *MB296B* did not affect 1-day memory at 32°C after 10×S training ($n$ = 9–10).

(F) Constitutive *NPFR* downregulation in PPL1-γ2α′1 neurons did not affect SFR after 10×S training ($n$ = 7).

(G) PPL1-α2α′2 DAN schematic.

(H) Acute *NPFR* downregulation in PPL1-α2α′2 neurons targeted by *MB058B* impaired 1-day memory after 10×S training ($n$ = 8).

(I) Constitutive *NPFR* downregulation in PPL1-α2α′2 neurons abolished the 10×S-induced decrease in SFR ($n$ = 7–9).

(J) PPL1-α3 DAN schematic.

(K) Acute *NPFR* downregulation in PPL1-α3 neurons targeted by *MB630B* impaired 1-day memory after 10×S training ($n$ = 10). (L) Constitutive *NPFR* downregulation in PPL1-α3 neurons showed a trend toward increased SFR after 10×S training ($p$ = 0.0522, $n$ = 5–7).

(M) Memory was unaffected after 10×S training when *NPFR RNAi* was not induced in these flies at 20°C ($n$ = 8).

(N) Learning was unaffected after 1× training when *NPFR RNAi* was induced in these flies at 32°C for 5 days ($n$ = 8–11).

(O) We observed elevated 3-h memory after 1× training when *NPFR RNAi* was induced in PPL1-α2α′2 but not in PPL1-α3 neurons ($n$ = 8).

(P) Surprisingly, we found the same pattern of 3-h memory after 1× training when *NPFR RNAi* was not induced in these flies at 20°C ($n$ = 7–8). Temperature control schedules are indicated (top). Box-and-whisker plots show the range of individual data points (whiskers), interquartile spread (box), median (bisecting line), and mean (+). Electrophysiology (Ephy) was measured 1–6 h after training. t tests were used for all comparisons except (I, M–P), compared using ANOVA and SNK when significant (I, O, P). *$p$ < 0.05; **$p$ < 0.01; ***$p$ < 0.001. See also Figure S2.

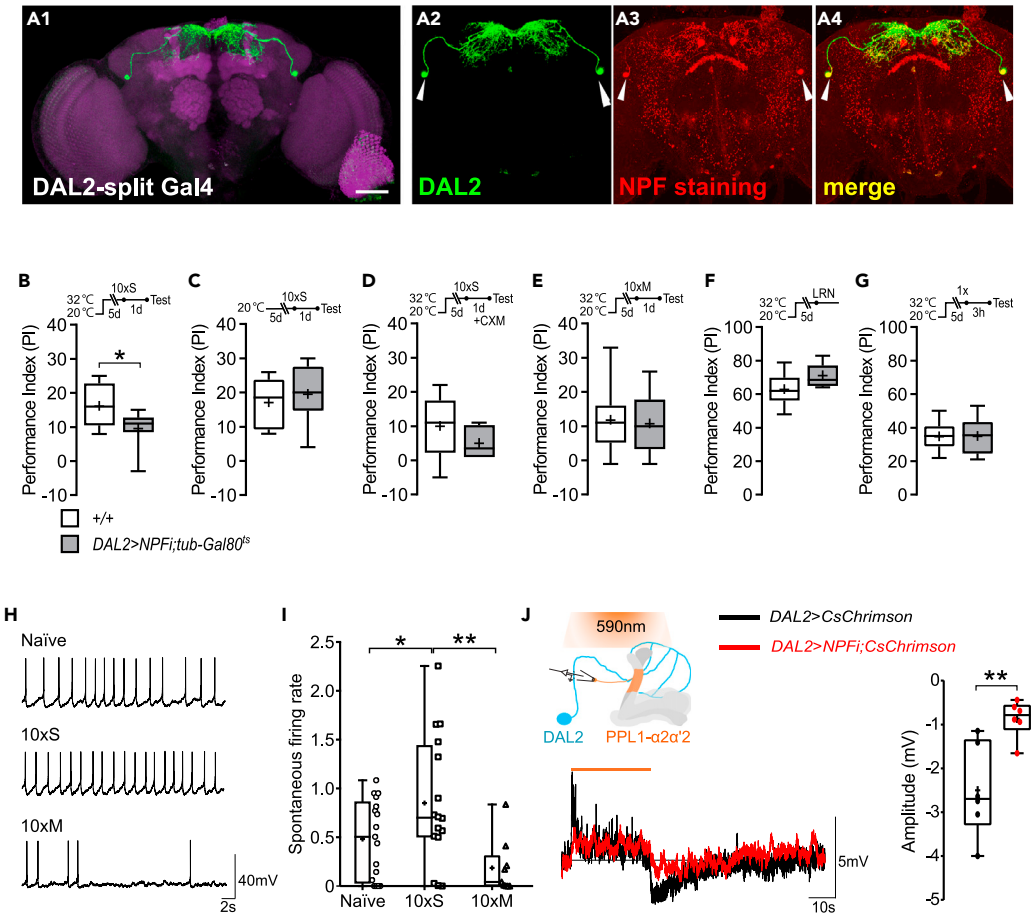


**Figure 4. Training-induced NPF signaling from DAL2 neurons inhibits PPL1 DANs**

(A1–A4) (A1) DAL2 neuron-specific split-*Gal4* expression of *mCD8::GFP* (green), counterstained with anti-DLG immunostaining (magenta). Scale bar, 50 μm. (A2) *DAL2* > *mCD8::GFP* expression (green) in DAL2 neurons (arrow heads). (A3) NFP immunostaining (red). (A4) Merged image showing co-localization of typical *Gal4* and strong NPF signals in DAL2 neurons.

(B) Adult-stage-specific downregulation of *NPF* targeted to DAL2 neurons in *DAL2* > *UAS-NPFi*; *tub-Gal80$^{ts}$* flies impaired 1-day memory after 10×S training ($n$ = 8). Flies were raised at 20°C and transferred to 32°C for 5 days before training to remove *tub-Gal80$^{ts}$* inhibition of Gal4.

(C) Memory was unaffected after 10×S when *NPF RNAi* was not induced in these flies at 20°C ($n$ = 8).

(D) LTM reduction after acute *NPF* downregulation in DAL2 neurons was not further impaired by CXM feeding ($n$ = 10).

(E) Acute *NPR* downregulation in DAL2 neurons had no effect on 1-day memory after 10×M training ($n$ = 10).

(F) The same manipulation did not affect learning after 1× training ($n$ = 8–10).

(G) Similarly, this manipulation did not affect 3-h memory after 1× training ($n$ = 6–8).

(H) Representative traces of spontaneous firing in DAL2 neurons of naïve fly and flies after 10×S and 10×M.

(I) SFR of DAL2 neurons was higher after 10×S training in comparison with naïve flies and flies after 10×M ($n$ = 9–17).

(J) Schematic illustration of electrophysiological recording from a PPL1-α2α′2 DAN and concurrent photoactivation of DAL2 neurons (up). Typical traces from PPL1-α2α′2 DANs recorded in *DAL2* > *CsChrimson* flies (black) and *DAL2* > *NPFi;CsChrimson* flies (red) upon 590 nm photoactivation for 30 s (bar) (down). Excitation of DAL2 neurons by photoactivation of CsChrimson induced prolonged hyperpolarization in PPL1-α2α′2 DANs (black), which was reduced by downregulating *NPF* and NPF signaling from DAL2 neurons (red) ($n$ = 6) (right). Temperature control schedules are indicated (top). Box-and-whisker plots show the range of individual data points (whiskers), interquartile spread (box), median (bisecting line), and mean (+). t tests were used for all comparisons except (I), compared using ANOVA and SNK. *$p < 0.05$; **$p < 0.01$. See also Figure S4.

dorsofrontal protocerebrum (SDFP) (Figure S3E). Although this proximity to PPL1 DANs suggested their candidacy as the presynaptic neurons (Figure S3D), we did not identify synaptic connections between them in the latest flyEM datasets (Scheffer et al., 2020) (Figures S3F and S3G; Data S1). To examine the role of DAL2 neurons in conditioned behavior we first generated a split-*Gal4* driver to target them (*DAL2*); this was derived from the genetic intersection of *NPF* and *VT26999* (Figures S3A and S3B), which has specific and exclusive expression in DAL2 neurons (Figure 4A1). We confirmed the specificity of the DAL2 split-*Gal4* driver with NPF immunostaining and showed clear co-localization (Figure 4A4).

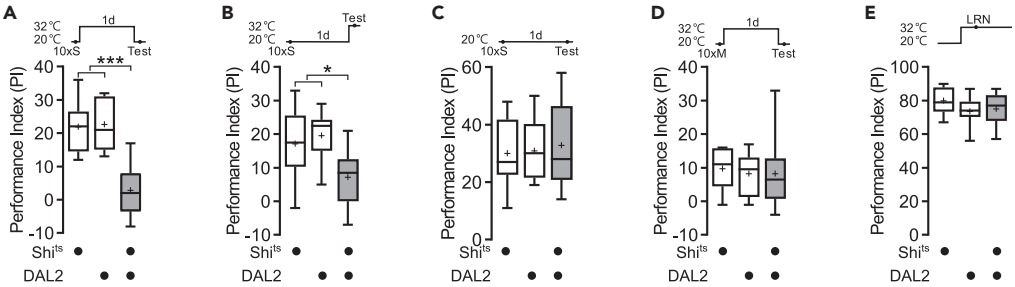


**Figure 5. Aversive LTM consolidation and retrieval requires DAL2 neuron output**

(A) Blocking output from DAL2 neurons in *DAL2* > *UAS-shi$^{ts}$* flies at 32°C during consolidation impaired 1-day memory after 10×S training ($n$ = 7–12).

(B) Similarly, blocking output from DAL2 neurons in these flies at 32°C during retrieval impaired 1-day memory after 10×S training ($n$ = 8–10).

(C) Memory was unaffected in these flies after 10×S when DAL2 neuron output was not blocked at 20°C ($n$ = 8–10).

(D) Blocking output from DAL2 neurons at 32°C during consolidation had no effect on 1-day memory after 10×M training ($n$ = 8–12).

(E) This same manipulation also did not affect learning after 1× training ($n$ = 8). Flies were raised at 20°C and transferred to 32°C for temporal control of the *UAS-shi$^{ts}$* transgene. Temperature control schedules are indicated (top). Box-and-whisker plots show the range of individual data points (whiskers), interquartile spread (box), median (bisecting line), and mean (+). ANOVA was used for all comparisons, SNK when significant (A and B). *p < 0.05; **p < 0.01; ***p < 0.001.

Next, we used *DAL2* to test whether adult-stage specific DAL2-targeted RNAi downregulation of NPF had an influence on memory. As in previous experiments, temporal control of the *UAS-NPFi* transgene was enabled using *tub-Gal80$^{ts}$*. We observed impaired 1-day LTM after 10×S training at 32°C ($p < 0.05$) (Figure 4B) but not at 20°C (Figure 4C). This impairment appeared to be complete, because 1-day memory was not further reduced by systemic feeding with CXM (Figure 4D). Moreover, NPF downregulation at 32°C was specific to LTM because we saw no effects on 1-day ARM after 10×M training (Figure 4E), on learning after 1× (Figure 4F), or on 3-h ITM after 1× training (Figure 4G).

We then tested whether DAL2 neuron activity differed among naïve and trained flies using whole-cell recordings. Post-training activity of DAL2 neurons was elevated by 10×S training in comparison with naïve flies and flies after 10×M training ($p < 0.05$) (Figures 4H and 4I), indicating that NPF release from these neurons was activity-dependent and specific to LTM. To test if DAL2 neurons directly regulate PPL1 DANs by releasing NPF, we targeted expression of the *CsChrimson* transgene, encoding a light-gated cation channel to DAL2 neurons (Klapoetke et al., 2014). By exciting CsChrimson in DAL2 neurons with light (590 nm), we recorded induced depolarized postsynaptic responses in PPL1-α2α′2 DANs followed by long-lasting hyperpolarization (Figure 4J). These responses were not observed in control flies without *CsChrimson* expression (Figure S4). The slow and prolonged dynamics of this hyperpolarization fit the temporal characteristics of neuropeptide release (Rao et al., 2001). RNAi knockdown of NPF in DAL2 neurons reduced this hyperpolarization, indicating that induction in PPL1-α2α′2 DANs was mediated by NPF signaling from DAL2 neurons (Figure 4J). Taken together, these results show that DAL2 neurons inhibit PPL1 DANs by the activity-dependent and spaced-training-specific release of NPF that is required for the consolidation of aversive LTM.

## Aversive LTM consolidation and retrieval requires DAL2 neuron output

Our results to this point demonstrate that DAL2 neurons may be considered part of the memory circuit in *Drosophila*. For a more complete understanding of their role in aversive olfactory memory consolidation, we blocked their output signals by targeting the *shi$^{ts}$* transgene to DAL2 neurons and examined the effects on different memory processes (Figure 5). Blocking DAL2 signaling during consolidation or retrieval impaired 1-day memory after 10×S training in flies expressing *shi$^{ts}$* at a restrictive temperature (32°C) in comparison with flies carrying either the *DAL2-Gal4* or *shi$^{ts}$* transgenes alone ($p < 0.05$) (Figures 5A and 5B) or in 10×S-trained flies maintained at a permissive temperature (20°C) throughout the experiment (Figure 5C). This impairment was specific to LTM because 1-day ARM after 10×M training (Figure 5D) and learning immediately after 1× training (Figure 5E) were not affected in flies expressing *shi$^{ts}$* at 32°C. These observations indicate that DAL2 neuron output is specifically involved in LTM consolidation and retrieval.


**Figure 6. Model: NPF inhibits DAN interference for LTM consolidation**

Persistent post-training activity of PPL1-α2α′2 and -α3 DANs interfere with LTM consolidation (left). DAL2 neurons are activated by 10×S training and release NPF. NPF inhibits interfering post-training activity of PPL1-α2α′2 and -α3 DANs allowing LTM consolidation (right).

## DISCUSSION

Repetitive or periodic events are more likely to be consolidated as LTM (Carew et al., 1972; Tully et al., 1994; Ebbinghaus, 2013). Consolidation begins immediately after learning, when post-training activities of various neurons persistently affect the integrity of new memory (Berry et al., 2018). Spaced training not only initiates cellular consolidation (Pagani et al., 2009) but here we showed that it also activates an inhibitory circuit mechanism to suppress post-training activity that interferes with LTM. Aversive LTM was either blocked or enhanced by up- or downregulation of DAN activity, respectively (Figure 1). Upstream NPF signaling inhibited post-training activity of these neurons during LTM consolidation (Figure 2). Only two of the four DAN types (PPL1-α2α′2s and PPL1-α3) were NPF responsive and gated LTM formation in this way (Figure 3). Then, we identified NPF-positive DAL2 neurons and showed their activity, and release of NPF in response to 10×S training inhibited PPL1-α2α′2s and -α3 neurons, enabling the consolidation and retrieval of aversive LTM (Figures 4 and 5). In sum, we found that spaced-training-induced NPF release from a single pair of DAL2 neurons inhibited post-training activity of PPL1-α2α′2 and PPL1-α3 DANs to ensure LTM consolidation. Our study establishes a memory model in which spaced-training-induced NPF signaling provides a disinhibitory gate required for aversive LTM consolidation in *Drosophila* (Figure 6).

### Persistent DAN activity in LTM formation

DAN signaling of reinforcement during olfactory learning has been well established (Waddell, 2013). Recent studies that highlight persistent post-training DAN activity have revealed additional regulatory roles during memory consolidation for both appetitive and aversive LTM (Berry et al., 2012; Plaçais et al., 2012; Ichinose et al., 2015). For appetitive LTM, the persistent post-training activity of PAM-α1 DANs is required to sustain the recurrent loop (KC → MBON → PAM → KC) during the consolidation process (Ichinose et al., 2015). In addition, the post-training activity of PPL1-γ1pedc DANs is initially required for but later suppresses appetitive LTM formation, whereas GABAergic MVP2 neuron inhibition of PPL1-γ1pedc DANs promotes appetitive LTM (Pavlowsky et al., 2018). For aversive LTM, blocking most of the PPL1 DANs at once resulted in either impaired or enhanced LTM. The outcome depended on whether inhibition occurred during the early stage (Plaçais et al., 2012) or throughout consolidation (Figure 1), respectively. Notwithstanding the varied drivers and training protocols used across studies, the seemingly contradictory results are more likely attributed to signaling differences among distinct types of PPL1 DANs during different windows of time in consolidation. Spaced-training-induced $Ca^{2+}$ oscillations with higher synchrony in PPL1-γ1pedc and -γ2α′1 DANs have been correlated with a switching of aversive ARM to LTM (Plaçais et al., 2012). Their activity erodes transient memory while promoting LTM (Berry et al., 2012, Plaçais et al., 2012). In contrast, here we showed that post-training PPL1-α2α′2 and -α3 DAN activity interfered with aversive LTM consolidation. The seemingly contradictory role of PPL1 DANs in regulating aversive LTM was clarified with cell-type-specific manipulation in this study. Based on these data we suggest there are two mechanisms acting through different PPL1 DANs. PPL1-γ1pedc and -γ2α DANs facilitate LTM initially, whereas PPL1-α2α′2 and -α3 DANs inhibit LTM later.

The origin of persistent PPL1 DAN activity has not been examined; however, we suggest two plausible explanations. Endogenous signals relayed by upstream elements (i.e., recurrent loops or pacemaker neurons) may induce spontaneous DAN activity in the absence of identified environmental stimuli, providing homeostatic regulation of the memory circuit (Scaplen et al., 2021; Vaccaro et al., 2017). Alternatively, persistent PPL1 DAN activity may reflect spurious exogenous sensory input (i.e., unrelated to planned experiments), causing either proactive or retroactive interference (in a cognitive psychology context) that contributes to the erosion of memory (Postman and Underwood, 1973; Berry et al., 2015; Sabandal et al., 2021). As such, our observation

that spaced training regulates persistent PPL1 DAN activity may reflect either a temporary shift to a new homeostatic set point in the circuit, a silencing of interference signals to allow LTM formation, or perhaps both.

### NPF signaling to DANs in systems consolidation

Systems memory consolidation implies that relevant processes occur simultaneously or sequentially among and between neurons in specific circuits and in different brain regions (Dubnau and Chiang, 2013). Biochemical consolidation has been shown in KCs and in the paired DAL neurons (Chen et al., 2012; Huang et al., 2012; Cervantes-Sandoval et al., 2013; Lee et al., 2018; Miyashita et al., 2018). Activity in several other neuron groups such as MBONs and serotonergic projection neurons (SPNs) is also required for protein-synthesis-dependent LTM (Séjourné et al., 2011; Pai et al., 2013; Bouzaiane et al., 2015; Wu et al., 2017; Scheunemann et al., 2018). Here, we showed that DAL2 neurons participate in the *Drosophila* memory circuit (Figure 4). Output from these neurons was required for the consolidation and retrieval of aversive LTM, as was evident by the elimination of these functions after blocking output with $shi^{ts}$ induction (Figure 5). However, thermogenetic inactivation of vesicle recycling with $shi^{ts}$ may potentially inhibit neurotransmission and neuropeptide release, which are both mediated by dynamin, simultaneously (Wong et al., 2015). We showed that peptidergic signaling from DAL2 neurons disinhibits aversive LTM consolidation, yet the significance of spike-dependent neurotransmission in LTM formation remains to be resolved.

The balance between maintenance and loss of memory traces in what may be described as engram neurons influences memory retention (Davis and Zhong, 2017). Several studies suggest that the integrity of memory is largely a function of the inhibition of trace decay or forgetting (Berry et al., 2018). Alternatively and as noted earlier, memory reflects all experiences, including spurious events that may interfere with conditioning in otherwise well-controlled experiments (Postman and Underwood, 1973). These unidentified external stimuli or circuit mechanisms lead to post-training persistent activity of PPL1-α2α′2 and -α3 DANs, resulting in consolidation failure (Figures 3H and 3K, respectively). Therefore, the upstream regulation of these neurons is critical for LTM formation. We suggest that inhibition of persistent PPL1-α2α′2 and -α3 neuron activity during consolidation promotes engram integrity within the memory circuit and propose that dynamic DAL2 neuron signaling modulation of this process is integral to systems consolidation in *Drosophila*.

### NPF as a general regulator of LTM

LTM formation is influenced by motivation, energy metabolism, and sleep—all processes known to be modulated by NPF signaling (Krashes et al., 2009; Donlea et al., 2011; Chung et al., 2017; Plaçais et al., 2017; Dag et al., 2019; Chouhan et al., 2021). Previous studies linked NPF with appetitive memory due to its role in motivating food-seeking behavior (Tsao et al., 2018; Lin et al., 2019). Through inhibition of PPL1-γ1pedc DANs, an NPF-mediated hunger signal is required for establishing 3-h appetitive memory (Krashes et al., 2009). Unlike aversive LTM that requires multiple training sessions, odor-reward conditioning in one session is sufficient to form appetitive LTM (Krashes and Waddell, 2008). Intriguingly, starved flies express higher levels of NPF in DAL2 neurons (Williams et al., 2020) and can form aversive LTM with only one session of odor-shock conditioning as well (Hirano et al., 2013). Here we showed that NPF signaling in well-fed (*ad libitum*) flies is also required to form aversive LTM after 10×S training. Taken together, we propose that NPF is a general regulator of memory consolidation, disinhibiting both appetitive and aversive LTM mechanisms. Release of NPF in response to either starvation or spaced training can suppress disruptive post-training DAN activity and allow LTM to form. A recent study found that a requirement for sleep during LTM consolidation after appetitive conditioning is dependent on hunger state (Chouhan et al., 2021). Starved flies need NPF signaling for sleep-independent memory consolidation. Because DAN activity declines during sleep (Berry et al., 2015), NPF inhibition of these neurons may compensate for the need to sleep.

In this study we found that all four types of PPL1 DANs were sensitive to external NPF application (Figures 2B–2E), but we only observed NPFR-mediated LTM in PPL1-α2α′2 and -α3 DANs (Figure 3). NPF signaling is characterized by slow, widespread, and long-lasting neuropeptide release that does not target specific postsynaptic partner neurons, in comparison with action-potential-mediated synaptic transmission (van den Pol, 2012). Therefore, differential regulation of PPL1 DANs appears to be a function of NPFR expression and density in downstream membranes. This aligns with a recent report of higher NPFR mRNA expression in PPL1-α2α′2 and -α3 DANs than in PPL1-γ1pedc and -γ2α′1 DANs (Aso et al., 2019). These distinctions may support the encoding of different memory components in parallel. Consistent with our results, a previous study showed that PPL1-α2α′2 and -α3 DANs projecting to vertical MB elements modulated

LTM, whereas PPL1-γ1pedc and -γ2α′1 DANs projecting mainly to horizontal MB elements were necessary for STM (Aso and Rubin, 2016). Thus, different phases and forms of memories appear to be established and regulated in spatially distinct domains. This report establishes a relationship between NPF/DAL2 neurons, NPFR/PPL1 DANs, and aversive LTM. We cannot rule out the possibility that NPF might also modulate memory formation by signaling to KCs, MBONs, or other elements of the memory circuit. A full accounting of NPF influences on learning and memory remains to be clarified. Beyond the initial convergent signals required to activate memory consolidation mechanisms, here we demonstrate that additional signals required to suppress interfering post-training activity are equally important for establishing LTM.

### Limitations of the study

(1) We showed that NPF is inhibitory to four PPL1 DANs by applying 500 nM of synthetic NPF. However, we do not know the endogenous concentration of NPF in the *Drosophila* brain. Therefore, we also do not know whether experimental and endogenous concentrations of NPF result in the same level of hyperpolarization in PPL1 DANs. Also, hyperpolarization is likely caused by activating G-protein gated potassium channels through NPFRs. The amplitude of hyperpolarization may not faithfully reflect NPFR numbers in postsynaptic membranes. (2) We showed NPF signaling from DAL2 to PPL1 DANs is critical for LTM consolidation. Nevertheless, we cannot exclude the possibilities that NPF from DAL2 also affects other neurons and that PPL1 DANs receive NPF signals from other sources. Both undetermined upstream and downstream partners of PPL1 DANs and DAL2, respectively, may contribute to LTM modulation. From our perspective, this is an opportunity to test new hypotheses about the systems neuroscience of interference in learning. (3) In our electrophysiological recordings, we found that the spontaneous activity of the same DANs with the same experimental conditions varied among individuals. We cannot account for this variation but suggest that it may reflect the stochastic nature of normal DAN physiology in *Drosophila*.

## STAR★METHODS

Detailed methods are provided in the online version of this paper and include the following:

- KEY RESOURCES TABLE
- RESOURCE AVAILABILITY
  - Lead contact
  - Materials availability
  - Data and code availability
- EXPERIMENTAL MODEL AND SUBJECT DETAILS
- METHOD DETAILS
  - Generation of DAL2 split-Gal4 flies
  - Behavioral assay
  - Electrophysiology
  - Immunostaining
  - Identification of candidate DAL2 neurons from flyEM datasets
- QUANTIFICATION AND STATISTICAL ANALYSIS
- DATA AND SOFTWARE AVAILABILITY

## SUPPLEMENTAL INFORMATION

Supplemental information can be found online at https://doi.org/10.1016/j.isci.2021.103506.

## ACKNOWLEDGMENTS

We thank Josh Dubnau, Todd A. Schlenk, Barry J. Dickson, Ping Shen, Liqun Luo, Tzumin Lee, Kristin Scott, Yoshinori Aso, the Bloomington Drosophila Stock Center, and the Vienna Drosophila RNAi Center (VDRC) for fly stocks. This work was financially supported by the Brain Research Center under the Higher Education Sprout Project co-funded by the Ministry of Education and the Ministry of Science and Technology in Taiwan, Yushan Scholar Program from the Ministry of Education in Taiwan.

## AUTHOR CONTRIBUTIONS

K.-L.F., J.-Y.W., and A.-S.C. designed the experiments. K.-L.F., C.-C. Chen, and M.B.A. performed behavior experiments. J.-Y.W. performed electrophysiology experiments. K.-L.F. and H.-W.L. conducted imaging

experiments. C.-C. Charng identified candidate neurons from flyEM datasets. K.-L.F. and J.-Y.W. analyzed the data and wrote the first draft. S.D.B., T.T., C.-C.L., and A.-S.C. reviewed and edited the manuscript.

## DECLARATION OF INTERESTS

The authors declare no competing interests.

Received: June 28, 2021
Revised: September 13, 2021
Accepted: November 22, 2021
Published: December 17, 2021

## REFERENCES

Aso, Y., Hattori, D., Yu, Y., Johnston, R.M., Iyer, N.A., Ngo, T.-T.B., Dionne, H., Abbott, L.F., Axel, R., Tanimoto, H., et al. (2014). The neuronal architecture of the mushroom body provides a logic for associative learning. eLife *3*, e04577. https://doi.org/10.7554/eLife.04577.

Aso, Y., Herb, A., Ogueta, M., Siwanowicz, I., Templier, T., Friedrich, A.B., Ito, K., Scholz, H., and Tanimoto, H. (2012). Three dopamine pathways induce aversive odor memories with different stability. PLoS Genet. *8*, e1002768. https://doi.org/10.1371/journal.pgen.1002768.

Aso, Y., Ray, R.P., Long, X., Bushey, D., Cichewicz, K., Ngo, T.T., Sharp, B., Christoforou, C., Hu, A., Lemire, A.L., et al. (2019). Nitric oxide acts as a cotransmitter in a subset of dopaminergic neurons to diversify memory dynamics. Elife *8*, e49257. https://doi.org/10.7554/eLife.49257.

Aso, Y., and Rubin, G.M. (2016). Dopaminergic neurons write and update memories with cell-type-specific rules. Elife *5*, e16135. https://doi.org/10.7554/eLife.16135.

Berry, J.A., Cervantes-Sandoval, I., Chakraborty, M., and Davis, R.L. (2015). Sleep facilitates memory by blocking dopamine neuron-mediated forgetting. Cell *161*, 1656–1667. https://doi.org/10.1016/j.cell.2015.05.027.

Berry, J.A., Cervantes-Sandoval, I., Nicholas, E.P., and Davis, R.L. (2012). Dopamine is required for learning and forgetting in *Drosophila*. Neuron *74*, 530–542. https://doi.org/10.1016/j.neuron.2012.04.007.

Berry, J.A., Phan, A., and Davis, R.L. (2018). Dopamine neurons mediate learning and forgetting through bidirectional modulation of a memory trace. Cell Rep. *25*, 651–662.e655. https://doi.org/10.1016/j.celrep.2018.09.051.

Bouzaiane, E., Trannoy, S., Scheunemann, L., Plaçais, P.Y., and Preat, T. (2015). Two independent mushroom body output circuits retrieve the six discrete components of *Drosophila* aversive memory. Cell Rep. *11*, 1280–1292. https://doi.org/10.1016/j.celrep.2015.04.044.

Brown, M.R., Crim, J.W., Arata, R.C., Cai, H.N., Chun, C., and Shen, P. (1999). Identification of a *Drosophila* brain-gut peptide related to the neuropeptide Y family. Peptides *20*, 1035–1042. https://doi.org/10.1016/s0196-9781(99)00097-2.

Carew, T.J., Pinsker, H.M., and Kandel, E.R. (1972). Long-term habituation of a defensive withdrawal reflex in *aplysia*. Science *175*, 451–454. https://doi.org/10.1126/science.175.4020.451.

Cervantes-Sandoval, I., Chakraborty, M., MacMullen, C., and Davis, R.L. (2016). Scribble scaffolds a signalosome for active forgetting. Neuron *90*, 1230–1242. https://doi.org/10.1016/j.neuron.2016.05.010.

Cervantes-Sandoval, I., Davis, R.L., and Berry, J.A. (2020). Rac1 impairs forgetting-induced cellular plasticity in mushroom body output neurons. Front. Cell. Neurosci. *14*, 258. https://doi.org/10.3389/fncel.2020.00258.

Cervantes-Sandoval, I., Martin-Peña, A., Berry, J.A., and Davis, R.L. (2013). System-like consolidation of olfactory memories in *Drosophila*. J. Neurosci. *33*, 9846–9854. https://doi.org/10.1523/JNEUROSCI.0451-13.2013.

Chen, C.C., Wu, J.K., Lin, H.W., Pai, T.P., Fu, T.F., Wu, C.L., Tully, T., and Chiang, A.S. (2012). Visualizing long-term memory formation in two neurons of the *Drosophila* brain. Science *335*, 678–685. https://doi.org/10.1126/science.1212735.

Chouhan, N.S., Griffith, L.C., Haynes, P., and Sehgal, A. (2021). Availability of food determines the need for sleep in memory consolidation. Nature *589*, 582–585. https://doi.org/10.1038/s41586-020-2997-y.

Chung, B.Y., Ro, J., Hutter, S.A., Miller, K.M., Guduguntla, L.S., Kondo, S., and Pletcher, S.D. (2017). *Drosophila* neuropeptide F signaling independently regulates feeding and sleep-wake behavior. Cell Rep. *19*, 2441–2450. https://doi.org/10.1016/j.celrep.2017.05.085.

Dag, U., Lei, Z., Le, J.Q., Wong, A., Bushey, D., and Keleman, K. (2019). Neuronal reactivation during post-learning sleep consolidates long-term memory in *Drosophila*. Elife *8*, e42786. https://doi.org/10.7554/eLife.42786.

Davis, R.L., and Zhong, Y. (2017). The biology of forgetting-a perspective. Neuron *95*, 490–503. https://doi.org/10.1016/j.neuron.2017.05.039.

Dierick, H.A., and Greenspan, R.J. (2007). Serotonin and neuropeptide F have opposite modulatory effects on fly aggression. Nat. Genet. *39*, 678–682. https://doi.org/10.1038/ng2029.

Donlea, J.M., Thimgan, M.S., Suzuki, Y., Gottschalk, L., and Shaw, P.J. (2011). Inducing sleep by remote control facilitates memory consolidation in *Drosophila*. Science *332*, 1571–1576. https://doi.org/10.1126/science.1202249.

Dubnau, J., and Chiang, A.S. (2013). Systems memory consolidation in *Drosophila*. Curr. Opin. Neurobiol. *23*, 84–91. https://doi.org/10.1016/j.conb.2012.09.006.

Dubnau, J., Grady, L., Kitamoto, T., and Tully, T. (2001). Disruption of neurotransmission in *Drosophila* mushroom body blocks retrieval but not acquisition of memory. Nature *411*, 476–480. https://doi.org/10.1038/35078077.

Ebbinghaus, H. (2013). Memory: a contribution to experimental psychology. Ann. Neurosci. *20*, 155–156. https://doi.org/10.5214/ans.0972.7531.200408.

Handler, A., Graham, T.G.W., Cohn, R., Morantte, I., Siliciano, A.F., Zeng, J., Li, Y., and Ruta, V. (2019). Distinct dopamine receptor pathways underlie the temporal sensitivity of associative learning. Cell *178*, 60–75 e19. https://doi.org/10.1016/j.cell.2019.05.040.

Hige, T., Aso, Y., Modi, M.N., Rubin, G.M., and Turner, G.C. (2015). Heterosynaptic plasticity underlies aversive olfactory learning in *Drosophila*. Neuron *88*, 985–998. https://doi.org/10.1016/j.neuron.2015.11.003.

Himmelreich, S., Masuho, I., Berry, J.A., MacMullen, C., Skamangas, N.K., Martemyanov, K.A., and Davis, R.L. (2017). Dopamine receptor DAMB signals via Gq to mediate forgetting in *Drosophila*. Cell Rep. *21*, 2074–2081. https://doi.org/10.1016/j.celrep.2017.10.108.

Hirano, Y., Masuda, T., Naganos, S., Matsuno, M., Ueno, K., Miyashita, T., Horiuchi, J., and Saitoe, M. (2013). Fasting launches CRTC to facilitate long-term memory formation in *Drosophila*. Science *339*, 443–446. https://doi.org/10.1126/science.1227170.

Huang, C., Zheng, X., Zhao, H., Li, M., Wang, P., Xie, Z., Wang, L., and Zhong, Y. (2012). A permissive role of mushroom body alpha/beta core neurons in long-term memory consolidation in *Drosophila*. Curr. Biol. *22*, 1981–1989. https://doi.org/10.1016/j.cub.2012.08.048.

Ichinose, T., Aso, Y., Yamagata, N., Abe, A., Rubin, G.M., and Tanimoto, H. (2015). Reward signal in a recurrent circuit drives appetitive long-term memory formation. Elife *4*, e10719. https://doi.org/10.7554/eLife.10719.

Jefferis, G.S., Potter, C.J., Chan, A.M., Marin, E.C., Rohlfing, T., Maurer, C.R., Jr., and Luo, L. (2007). Comprehensive maps of Drosophila higher olfactory centers: spatially segregated fruit and pheromone representation. Cell *128*, 1187–1203. https://doi.org/10.1016/j.cell.2007.01.040.

Kacsoh, B.Z., Lynch, Z.R., Mortimer, N.T., and Schlenke, T.A. (2013). Fruit flies medicate offspring after seeing parasites. Science *339*, 947–950. https://doi.org/10.1126/science.1229625.

Klapoetke, N.C., Murata, Y., Kim, S.S., Pulver, S.R., Birdsey-Benson, A., Cho, Y.K., Morimoto, T.K., Chuong, A.S., Carpenter, E.J., Tian, Z., et al. (2014). Independent optical excitation of distinct neural populations. Nat. Methods *11*, 338–346. https://doi.org/10.1038/nmeth.2836.

Kondo, S., and Ueda, R. (2013). Highly improved gene targeting by germline-specific Cas9 expression in Drosophila. Genetics *195*, 715–721. https://doi.org/10.1534/genetics.113.156737.

Krashes, M.J., DasGupta, S., Vreede, A., White, B., Armstrong, J.D., and Waddell, S. (2009). A neural circuit mechanism integrating motivational state with memory expression in *Drosophila*. Cell *139*, 416–427. https://doi.org/10.1016/j.cell.2009.08.035.

Krashes, M.J., and Waddell, S. (2008). Rapid consolidation to a radish and protein synthesis-dependent long-term memory after single-session appetitive olfactory conditioning in *Drosophila*. J. Neurosci. *28*, 3103–3113. https://doi.org/10.1523/JNEUROSCI.5333-07.2008.

Lee, P.T., Lin, G., Lin, W.W., Diao, F., White, B.H., and Bellen, H.J. (2018). A kinase-dependent feedforward loop affects CREBB stability and long term memory formation. Elife *7*, e33007. https://doi.org/10.7554/eLife.33007.

Lin, H.-W., Chen, C.-C., de Belle, J.S., Tully, T., and Chiang, A.-S. (2021). CREBA and CREBB in two identified neurons gate long-term memory formation in *Drosophila*. Proc. Natl. Acad. Sci. U S A *118*. e2100624118. https://doi.org/10.1073/pnas.2100624118.

Lin, S., Senapati, B., and Tsao, C.H. (2019). Neural basis of hunger-driven behaviour in *Drosophila*. Open Biol. *9*, 180259. https://doi.org/10.1098/rsob.180259.

McGaugh, J.L. (1966). Time-dependent processes in memory storage. Science *153*, 1351–1358. https://doi.org/10.1126/science.153.3742.1351.

McGuire, S.E., Le, P.T., Osborn, A.J., Matsumoto, K., and Davis, R.L. (2003). Spatiotemporal rescue of memory dysfunction in Drosophila. Science *302*, 1765–1768. https://doi.org/10.1126/science.1089035.

Miyashita, T., Kikuchi, E., Horiuchi, J., and Saitoe, M. (2018). Long-term memory engram cells are established by c-Fos/CREB transcriptional cycling. Cell Rep. *25*, 2716–2728.e2713. https://doi.org/10.1016/j.celrep.2018.11.022.

Nairne, J.S., Thompson, S.R., and Pandeirada, J.N. (2007). Adaptive memory: survival processing enhances retention. J. Exp. Psychol. Learn Mem. Cogn. *33*, 263–273. https://doi.org/10.1037/0278-7393.33.2.263.

Pagani, M.R., Oishi, K., Gelb, B.D., and Zhong, Y. (2009). The phosphatase SHP2 regulates the spacing effect for long-term memory induction. Cell *139*, 186–198. https://doi.org/10.1016/j.cell.2009.08.033.

Pai, T.P., Chen, C.C., Lin, H.H., Chin, A.L., Lai, J.S., Lee, P.T., Tully, T., and Chiang, A.S. (2013). *Drosophila* ORB protein in two mushroom body output neurons is necessary for long-term memory formation. Proc. Natl. Acad. Sci. U S A *110*, 7898–7903. https://doi.org/10.1073/pnas.1216336110.

Pavlowsky, A., Schor, J., Plaçais, P.Y., and Preat, T. (2018). A GABAergic feedback shapes dopaminergic input on the *Drosophila* mushroom body to promote appetitive long-term memory. Curr. Biol. *28*, 1783–1793.e1784. https://doi.org/10.1016/j.cub.2018.04.040.

Perisse, E., Owald, D., Barnstedt, O., Talbot, C.B., Huetteroth, W., and Waddell, S. (2016). Aversive learning and appetitive motivation toggle feed-forward inhibition in the *Drosophila* mushroom body. Neuron *90*, 1086–1099. https://doi.org/10.1016/j.neuron.2016.04.034.

Perkins, K.L. (2006). Cell-attached voltage-clamp and current-clamp recording and stimulation techniques in brain slices. J. Neurosci. Methods *154*, 1–18. https://doi.org/10.1016/j.jneumeth.2006.02.010.

Plaçais, P.Y., de Tredern, E., Scheunemann, L., Trannoy, S., Goguel, V., Han, K.A., Isabel, G., and Preat, T. (2017). Upregulated energy metabolism in the *Drosophila* mushroom body is the trigger for long-term memory. Nat. Commun. *8*, 15510. https://doi.org/10.1038/ncomms15510.

Plaçais, P.Y., Trannoy, S., Isabel, G., Aso, Y., Siwanowicz, I., Belliart-Guerin, G., Vernier, P., Birman, S., Tanimoto, H., and Preat, T. (2012). Slow oscillations in two pairs of dopaminergic neurons gate long-term memory formation in *Drosophila*. Nat. Neurosci. *15*, 592–599. https://doi.org/10.1038/nn.3055.

Postman, L., and Underwood, B.J. (1973). Critical issues in interference theory. Mem. Cognit. *1*, 19–40. https://doi.org/10.3758/BF03198064.

Qin, H., Cressy, M., Li, W., Coravos, J.S., Izzi, S.A., and Dubnau, J. (2012). Gamma neurons mediate dopaminergic input during aversive olfactory memory formation in *Drosophila*. Curr. Biol. *22*, 608–614. https://doi.org/10.1016/j.cub.2012.02.014.

Rao, S., Lang, C., Levitan, E.S., and Deitcher, D.L. (2001). Visualization of neuropeptide expression, transport, and exocytosis in *Drosophila* melanogaster. J. Neurobiol. *49*, 159–172. https://doi.org/10.1002/neu.1072.

Reale, V., Chatwin, H.M., and Evans, P.D. (2004). The activation of G-protein gated inwardly rectifying K+ channels by a cloned *Drosophila* melanogaster neuropeptide F-like receptor. Eur. J. Neurosci. *19*, 570–576. https://doi.org/10.1111/j.0953-816x.2003.03141.x.

Sabandal, J.M., Berry, J.A., and Davis, R.L. (2021). Dopamine-based mechanism for transient forgetting. Nature *591*, 426–430. https://doi.org/10.1038/s41586-020-03154-y.

Scaplen, K.M., Talay, M., Fisher, J.D., Cohn, R., Sorkac, A., Aso, Y., Barnea, G., and Kaun, K.R. (2021). Transsynaptic mapping of *Drosophila* mushroom body output neurons. Elife *10*, e63379. https://doi.org/10.7554/eLife.63379.

Scheffer, L.K., Xu, C.S., Januszewski, M., Lu, Z., Takemura, S.Y., Hayworth, K.J., Huang, G.B., Shinomiya, K., Maitlin-Shepard, J., Berg, S., et al. (2020). A connectome and analysis of the adult *Drosophila* central brain. Elife *9*, e57443. https://doi.org/10.7554/eLife.57443.

Scheunemann, L., Plaçais, P.Y., Dromard, Y., Schwarzel, M., and Preat, T. (2018). Dunce phosphodiesterase acts as a checkpoint for *Drosophila* long-term memory in a pair of serotonergic neurons. Neuron *98*, 350–365.e355. https://doi.org/10.1016/j.neuron.2018.03.032.

Schwaerzel, M., Monastirioti, M., Scholz, H., Friggi-Grelin, F., Birman, S., and Heisenberg, M. (2003). Dopamine and octopamine differentiate between aversive and appetitive olfactory memories in *Drosophila*. J. Neurosci. *23*, 10495–10502.

Séjourné, J., Plaçais, P.Y., Aso, Y., Siwanowicz, I., Trannoy, S., Thoma, V., Tedjakumala, S.R., Rubin, G.M., Tchenio, P., Ito, K., et al. (2011). Mushroom body efferent neurons responsible for aversive olfactory memory retrieval in *Drosophila*. Nat. Neurosci. *14*, 903–910. https://doi.org/10.1038/nn.2846.

Shuai, Y., Lu, B., Hu, Y., Wang, L., Sun, K., and Zhong, Y. (2010). Forgetting is regulated through Rac activity in *Drosophila*. Cell *140*, 579–589. https://doi.org/10.1016/j.cell.2009.12.044.

Tonegawa, S., Morrissey, M.D., and Kitamura, T. (2018). The role of engram cells in the systems consolidation of memory. Nat. Rev. Neurosci. *19*, 485–498. https://doi.org/10.1038/s41583-018-0031-2.

Tsao, C.H., Chen, C.C., Lin, C.H., Yang, H.Y., and Lin, S. (2018). *Drosophila* mushroom bodies integrate hunger and satiety signals to control innate food-seeking behavior. Elife *7*, e35264. https://doi.org/10.7554/eLife.35264.

Tully, T., Preat, T., Boynton, S.C., and Del Vecchio, M. (1994). Genetic dissection of consolidated memory in *Drosophila*. Cell *79*, 35–47. https://doi.org/10.1016/0092-8674(94)90398-0.

Vaccaro, A., Issa, A.R., Seugnet, L., Birman, S., and Klarsfeld, A. (2017). *Drosophila* clock is required in brain pacemaker neurons to prevent premature locomotor aging independently of its circadian function. PLoS Genet. *13*, e1006507. https://doi.org/10.1371/journal.pgen.1006507.

van den Pol, A.N. (2012). Neuropeptide transmission in brain circuits. Neuron *76*, 98–115. https://doi.org/10.1016/j.neuron.2012.09.014.

Viswanath, V., Story, G.M., Peier, A.M., Petrus, M.J., Lee, V.M., Hwang, S.W., Patapoutian, A., and Jegla, T. (2003). Opposite thermosensor in fruitfly and mouse. Nature *423*, 822–823. https://doi.org/10.1038/423822a.

Waddell, S. (2013). Reinforcement signalling in *Drosophila*; dopamine does it all after all. Curr. Opin. Neurobiol. *23*, 324–329. https://doi.org/10.1016/j.conb.2013.01.005.

Williams, M.J., Akram, M., Barkauskaite, D., Patil, S., Kotsidou, E., Kheder, S., Vitale, G., Filaferro, M., Blemings, S.W., Maestri, G., et al. (2020). CCAP regulates feeding behavior via the NPF pathway in *Drosophila* adults. Proc. Natl. Acad. Sci. U S A *117*, 7401–7408. https://doi.org/10.1073/pnas.1914037117.

Wong, M.Y., Cavolo, S.L., and Levitan, E.S. (2015). Synaptic neuropeptide release by dynamin-dependent partial release from circulating vesicles. Mol. Biol. Cell *26*, 2466–2474. https://doi.org/10.1091/mbc.E15-01-0002.

Wu, J.K., Tai, C.Y., Feng, K.L., Chen, S.L., Chen, C.C., and Chiang, A.S. (2017). Long-term memory requires sequential protein synthesis in three subsets of mushroom body output neurons in *Drosophila*. Sci. Rep. *7*, 7112. https://doi.org/10.1038/s41598-017-07600-2.

## STAR★METHODS

### KEY RESOURCES TABLE

| REAGENT or RESOURCE | SOURCE | IDENTIFIER |
|---|---|---|
| Antibodies | | |
| mouse 4F3 anti-DLG antibody | Hybridoma Bank, UI | Cat. 4F3 anti-discs large; RRID:AB_528203 |
| rabbit anti-NPF antibody | RayBiotech | Cat. RB-19-0001-200; RRID:AB_11219226 |
| rabbit anti-NPFR-C | RayBiotech | Cat. RB-19-0002-20 |
| mouse anti-CD4 | Invitrogen | Cat. MA5-12259; RRID:AB_10989399 |
| rabbit anti-HA | Invitrogen | Cat. ab9110; RRID:AB_307019 |
| biotinylated goat anti-mouse IgG | Invitrogen | Cat. B2763; RRID:AB_1500659 |
| biotinylated goat anti-rabbit IgG | Invitrogen | Cat. B2770; RRID:AB_10375717 |
| goat anti-mouse IgG-Alexa546 | Invitrogen | Cat. A-11003; RRID:AB_2534071 |
| Chemicals, peptides, and recombinant proteins | | |
| 3-octanol (OCT) | Sigma-Aldrich | Cat. 218405 |
| 4-methylcyclohexanol (MCH) | Sigma-Aldrich | Cat. 153095 |
| Cycloheximide (cxm) | Sigma-Aldrich | Cat. C7698 |
| Neuropeptide F | Mission Biotech | N/A |
| Experimental models: Organisms/strains | | |
| Canton-S w1118(iso1CJ) | Tully et al. (1994) | N/A |
| MB504B-SplitGal4 | Aso et al. (2014) | RRID:BDSC_68329 |
| UAS-TrpA1 | From Paul Garrity | RRID:BDSC_26263 |
| UAS-Shibire$^{ts}$ | Dubnau et al. (2001) | Flybase: FBtp0013545 |
| MB320C-SplitGal4 | Aso et al. (2014) | RRID:BDSC_68253 |
| MB296B-SplitGal4 | Aso et al. (2014) | RRID:BDSC_68308 |
| MB058B-SplitGal4 | Aso et al. (2014) | RRID:BDSC_68278 |
| MB630B-SplitGal4 | Aso et al. (2014) | RRID:BDSC_68334 |
| TubP-GAL80[ts] | BDSC | RRID:BDSC_7019 |
| UAS-NPFR-RNAi(X) | Kacsoh et al. (2013) | N/A |
| UAS-NPF-RNAi(X) | Kacsoh et al. (2013) | N/A |
| UAS-mCD8::GFP(II) | BDSC | RRID:BDSC_5137 |
| UAS-mCD8::GFP(III) | BDSC | RRID:BDSC_5130 |
| VT26999-Gal4 | From Barry J. Dickson | N/A |
| NPF-GAL4(II) | Dierick and Greenspan (2007) | N/A |
| UAS-syt::HA(III) | Jefferis et al. (2007) | N/A |
| UAS-Dscam::GFP(x) | From Tzumin Lee | N/A |
| *UAS-mCD4::GFP$_{1-10}$ (III)* | From Kristin Scott | N/A |
| lexAop-mCD4::GFP11 (III) | From Kristin Scott | N/A |
| NPF-T2A-Gal4DBD (III) | This study | N/A |
| VT026999-p56AD (III) | This study | N/A |
| UAS-CsChrimson::mVenus (X) | BDRC | RRID:BDSC_55134 |
| LexAop-rCD2::GFP (III) | From Tzumin Lee | N/A |
| GMR82C10-lexA (II) | Janelia Farm | RRID:BDSC_54981 |
| VT45661-LexA (II) | From Yoshinori Aso | N/A |

(*Continued on next page*)

*Continued*

| REAGENT or RESOURCE | SOURCE | IDENTIFIER |
|---|---|---|
| Software and algorithms | | |
| GraphPad Prism 9 | GraphPad Software, San Diego CA, 2007 | http://www.graphpad.com/ |
| Clamplex 10 | Molecular Device, Sunnyvale, CA | https://www.moleculardevices.com/ |
| Clampfit 10 | Molecular Device, Sunnyvale, CA | https://www.moleculardevices.com/ |
| ZEISS Efficient Navigation (ZEN) | Zeiss, Jena, Germany | https://www.zeiss.com |

## RESOURCE AVAILABILITY

### Lead contact

Further information and requests for resources and reagents should be directed to and will be fulfilled by the lead contact, Ann-Shyn Chiang (aschiang@life.nthu.edu.tw).

### Materials availability

All stable reagents generated in this study are available from the Chiang Lab without restriction.

### Data and code availability

- Data have been deposited at Mendeley Data and are publicly available as of the date of publication (DOIs: https://doi.org/10.17632/g4rdw8rvxf.1).
- This paper does not report original code.
- Any additional information required to reanalyze the data reported in this paper is available from the lead contact upon request.

## EXPERIMENTAL MODEL AND SUBJECT DETAILS

*Drosophila melanogaster* wild-type strain *Canton-S* $w^{1118}$ (*iso1CJ*) and mutant flies were raised on standard corn meal/yeast/agar food at 20 ± 2°C and 70 ± 10% relative humidity on a 12 h:12 h light:dark cycle. The fly lines used are listed in the Key Resource Table. *Gal4* drivers for expressing the genes of interest included: *MB504B*, *MB320C*, *MB296B*, *MB058B*, and *MB630B* (from Janelia Farm, VA, USA.) for expression in PPL1-DANs; *NPF-Gal4(II)* (gift from Ping Shen), *VT26999-Gal4* (gift from Barry J. Dickson), and *DAL2 split-Gal4* (generated by WellGenetics in this study; see protocol below) for expression in DAL2 neurons. *LexA* driver for expression in PPL1-α2α′2 neurons: *GMR82C10-lexA* (from BDSC). RNAi for down-regulating target genes: *UAS-NPFR-RNAi(X)* and *UAS-NPF-RNAi(X)* (gift from Todd A. Schlenke).

## METHOD DETAILS

### Generation of DAL2 split-Gal4 flies

*NPF-T2A-Gal4DBD::Zip* flies and *VT026999-p65AD@attP2* were generated to create the *DAL2* split-*Gal4* line. CRISPR-mediated mutagenesis was performed by WellGenetics Inc (Taipei, Taiwan) (Kondo and Ueda, 2013). In brief, the gRNA sequence *ATGAGTTAGTGACGTTGCCA[TGG]* was cloned into a *U6* promoter plasmid(s). Cassette *T2A-Gal4DBD-RFP* containing *T2A*, Gal4DBD, two *loxP* sites, *Hsp70Ba 3′UTR*, 3x *P3-RFP* and two homology arms were cloned into *pUC57-Kan* as donor template for repair. *NPF/CG10342*-targeting gRNAs and *hs-Cas9* were supplied in DNA plasmids, together with donor plasmid for microinjection into embryos of control strain $w^{1118}$. $F_1$ flies carrying selection marker of 3x *P3-RFP* were further validated by genomic PCR and sequencing. CRISPR generated a break in *NPF/CG10342* and was replaced by cassette *T2A-Gal4DBD-RFP*. For *VT026999-p65AD@attP2*: PCR genomic fragment *VT026999* from genomic DNA of $w^{1118}$ and cloned into *pENTR*™ using Directional TOPO Cloning (Thermo, WLM, MA, USA, K2400-20). *VT026999* was then transferred from *pENTR/D-TOPO* to destination clone *pBPp65ADZpUw* (Addgene, Watertown, MA, USA #26234) using Gateway™ LR Clonase (Thermo 11791-020). Two transgenes were then recombined onto the same chromosome.

### Behavioral assay

Olfactory associative conditioning was conducted with well-established Pavlovian conditioning procedure (Tully et al., 1994). One day before conducting behavioral assays, flies were transferred into fresh food-contained

bottles with tissue paper as to make the flies clear and dry. Memory performance was evaluated by training 3- to 7-day-old flies. In all experiments, odorants used were 0.15% of 3-octanol (OCT) (Sigma, St. Louis, MO, USA) and 0.1% of 4-methylcyclohexanol (MCH) (Sigma). Each experiment consisted of two groups of approximately 80–100 flies, each of which was conditioned with one of these odors (conditioned stimuli, CS). Flies were loaded into the training chamber. After 90 s of acclimatization, flies were exposed for 60 s to the $CS^+$ paired with twelve 1.5 s pulses of 70–75 V dc electric shock at 5 s inter-pulse intervals (unconditioned stimulus, US). After the presentation of $CS^+$, the training chamber was flushed with fresh air for 45 s and then flies were exposed to the $CS^-$ without shock for 60 s. This procedure constituted one training cycle. To evaluate the memory retention, the trained flies were placed into an elevator-like chamber and transported to the choice point where converging air currents delivered $CS^+$ and $CS^-$ odors from opposite arms of T-maze. After 120 s the elevator-like chamber was slid out of register, trapping flies in their respective arms of the T maze. They were subsequently anesthetized and counted. A calculated performance index (PI) = $[(N_{CS-} - N_{CS+})/(N_{CS-} + N_{CS+})] \times 100$. To eliminate possible biases originating from the T-maze, naïve odor preferences or other non-associative sources, the PI of two complimentary experiments were averaged to give a single PI for both halves of the experiment. One cycle training (1x) was conducted through manual operation of T-maze, while 10x spaced (10xS) and 10x massed (10xM) training were conducted using automated "robotrainers", in which odor and shock delivery was controlled by computer software. 10xS training was comprised of 10 training sessions separated by 10 min rest intervals, whereas 10xM training was comprised of the same total amount of training but without rest intervals. During the memory retention interval, trained flies were placed in food vials and kept flat in an incubator at 20°C or 32°C, depending on the experimental protocol. For *TrpA1* and $shi^{ts}$ experiments, flies were reared in 20°C and later exposed to 32°C, depending on the experimental protocol. To manipulate neurons during memory consolidation, flies were moved to 30–32°C immediately after training and then back to 20°C for 30 min before testing. To block neuronal output during retrieval, flies were moved to 32°C for 30 min before testing. All RNAi down-regulation in behavior experiments was specifically induced in adult flies with the TARGET system (McGuire et al., 2003) except for *NPFRi-shi*$^{ts}$ co-expression. In these experiments, flies were reared at 20°C throughout development, then kept at 30–32°C for 5 days before training and through memory consolidation to fully induce RNAi expression. To block protein synthesis, flies were fed 35 mM cycloheximide (Sigma) in 5% glucose overnight, trained as described above and returned to regular food until testing.

## Electrophysiology

To perform *ex vivo* whole-cell recording, the brain was remove from the head and immobilized in oxygenized external saline containing the following (in mM): 103 NaCl, 3 KCl, 5 N-Tris(hydroxymethyl) methyl-2-aminoethane-sulfonic acid, 2 sucrose, 8 trehalose, 10 glucose, 26 $NaHCO_3$, 1 $NaH_2PO_4$, 1.5 $CaCl_2$, and 4 $MgCl_2$. The oxygenation and the pH was maintained by bubbling with 95% $O_2$/5% $CO_2$. The internal solution contained (in mM): 140 K-Aspartate*0.5$H_2O$, 10 HEPES, 1 KCl, 4 MgATP, 1 EGTA, 0.5 $Na_3GTP$, and 5 biocytin. The pH value of the internal solution was adjusted by KOH to ~7.3. The neurons of interest were identified by fluorescence expression and visual guidance using infrared differential interference contrast (IR-DIC) video microscopy (DAGE MTI IR-1000; Scientifica, Uckfield, UK) with a 40x water-immersion objective (Olympus, Tokyo, Japan). The spontaneous firing rate of DANs was recorded by cell-attached recording to prevent artificial mixture of cytosol and increased activities by poor sealing (Perkins, 2006). To prevent unnecessarily charging the cell membrane, command potential was clamped at the membrane potential which had no net current. The data was only analyzed when the cell-attached recording was stable for more than 5 minutes. After the cell-attached recording, the membrane was ruptured to allow the diffusion of biocytin. The cell type was confirmed by post-hoc staining. The representative traces are shown in Figure S2. For some unknown reason, cell-attached recording on DAL2s did not last long enough. Whole-cell recording was used instead on DAL2s for spontaneous firing rate recording. The electrophysiological recording was amplified and digitized by Multiclamp 700B and DigiData 1550B (Molecular Device, Sunnyvale, CA). The sampling rate was 10 kHz and low-pass filtered at 4 kHz. The data was analyzed by Clampfit 10 (Molecular Device, Sunnyvale, CA). *Drosophila melanogaster* NPF (amino acid sequence: SNSRPPRKNDVNTMADAYKFLQDLDTYYGDRARVRFamide; 86% pure) (Brown et al., 1999) synthesized by Mission Biotech (Taipei, Taiwan) was dissolved in the solvent composed of 30% acetonitrile/70% dd$H_2O$ for 1 mM as the stock solution. Therefore, for the experiments regarding to NPF application, equivalent solvent was added during the baseline.

## Immunostaining

Fly brains were dissected in phosphate-buffered saline (PBS) and immediately fixed in 4% paraformaldehyde at room temperature for 30 min. Subsequently, brain samples were transferred to penetration-blocking buffer

(PBS containing 2% Triton X-100 and 10% normal goat serum (NGS; Vector Laboratories, CA, USA) and degassed in a vacuum chamber to expel tracheal air before being incubated overnight at 4°C. Next, brain samples were incubated in PBST with primary antibodies at 4°C for 3–4 days, then in secondary antibodies at 4°C for 1 day, and finally in Alexa Fluor 635 (1:200, Invitrogen, Carlsbad, CA, USA) streptavidin at 4°C for 1 day. Samples were washed in washing buffer for 20 min three times after each step. Finally, the brain samples were directly cleared in FocusClearTM (CelExplorer, Hsinchu, Taiwan) and mounted between two cover slips separated by a spacer ring of ~200 μm in thickness. The primary antibodies used in this study were: (1) 1:20 mouse 4F3 anti-DLG antibody (Developmental Studies Hybridoma Bank, Univ. of Iowa), (2) 1:200 rabbit anti-NPF antibody (from RayBiotech, Peachtree Corners, GA, USA), (3) 1:200 rabbit anti-NPFR-C (from RayBiotech), and (4) 1:200 mouse anti-CD4, and rabbit anti-HA (from Invitrogen). Secondary antibodies: (1) 1:200 biotinylated goat anti-mouse IgG (B2763, Invitrogen), (2) 1:200 biotinylated goat anti-rabbit IgG (A10518, Invitrogen), and (3) 1:200 goat anti-mouse IgG fused with Alexa Fluor 546 (A11003, Invitrogen). Sample brains were imaged under a Zeiss LSM 710 confocal microscope with a 40X C-Apochromat water-immersion objective lens (N.A. value 1.2, working distance 220μm) (Zeiss, Jena, Germany).

### Identification of candidate DAL2 neurons from flyEM datasets

We warped DAL2 (npf-M-200004) neurons from FlyCircuit database to FlyEM hemibrain using python package navis-flybrains (https://github.com/schlegelp/navis, https://github.com/schlegelp/navis-flybrains) and probreg (https://github.com/neka-nat/probreg). Then, we compared the bounding box size of DAL2 with all neurons in FlyEM to generate the candidate list. Next, we compared the spatial innervation density and then manually identified candidate DAL2 neurons in FlyEM.

## QUANTIFICATION AND STATISTICAL ANALYSIS

Statistical analyses and graphs were done with GraphPad Prism 9 (San Diego, CA, USA). One-way ANOVA was used to compare data among three or more groups, followed by the Student-Newman-Keuls multiple comparisons test ($P < 0.05$). Unpaired Student's *t*-tests or Mann-Whitney *U*-tests were used to compared two relevant groups when data distributions were found to be normal or not, respectively (Anderson-Darling test). The sample sizes of individual experiments were indicated in the figure legend. In all figures, box-and-whisker plots show the range of individual data points (whiskers), interquartile spread (box), median (bisecting line), and mean (+). *, $P < 0.05$; **, $P < 0.01$; ***, $P < 0.001$.

## DATA AND SOFTWARE AVAILABILITY

GraphPad Prism 9 (San Diego, CA, USA)

Clamplex 10 (Molecular Device, Sunnyvale, CA, USA)

Clampfit 10 (Molecular Device, Sunnyvale, CA, USA)